

Dynamics of high-order solitons in the nonlocal nonlinear Schrödinger equations

Bo Yang, Yong Chen*

March 6, 2024

Abstract

A study of high-order solitons in three nonlocal nonlinear Schrödinger equations is presented, which includes the \mathcal{PT} -symmetric, reverse-time, and reverse-space-time nonlocal nonlinear Schrödinger equations. General high-order solitons in three different equations are derived from the same Riemann-Hilbert solutions of the AKNS hierarchy, except for the difference in the corresponding symmetry relations on the “perturbed” scattering data. Dynamics of general high-order solitons in these equations is further analyzed. It is shown that the high-order fundamental-soliton is always moving on several different trajectories in nearly equal velocities, and they can be nonsingular or repeatedly collapsing, depending on the choices of the parameters. It is also shown that the high-order multi-solitons could have more complicated wave structures and behave very differently from high-order fundamental solitons. More interesting is the high-order hybrid-pattern solitons, which are derived from combination of different size of block matrix in the Riemann-Hilbert solutions and thus they can describe a nonlinear interaction between several types of solitons.

1 Introduction

As an significant subject in many branches of nonlinear science, the integrable nonlinear wave equations and soliton theory has been studied for many years [1, 2, 3, 4, 5]. Most of the integrable equations are local equations, i.e., the solutions evolution depends only on the local solution value with its local space and time derivatives. Recently, a number of nonlocal integrable equations were found and triggered renewed interest in integrable systems. The first such nonlocal equation was the \mathcal{PT} -symmetric nonlinear Schrödinger (NLS) equation[6, 7]:

$$iq_t(x, t) = q_{xx}(x, t) + 2q^2(x, t)q^*(-x, t), \quad (1)$$

where asterisk $*$ represents complex conjugation. For this equation, the evolution of the solution at location x depends both on the local position x and the distant nonlocal position $-x$. This implies that the states of the solution at distant opposite locations are directly related, reminiscent of quantum entanglement in pairs of particles. This nonlocal integrable equation is distinctly different from local equations, which makes it mathematically interesting. In the view of potential applications, this equation was linked to an unconventional system of magnetics[8]. In addition, since equation (1) is parity-time (\mathcal{PT}) symmetric, it is related to the concept of \mathcal{PT} -symmetry, which is a hot research area of contemporary physics[9].

Nonlocal equation (1) was actively investigated[6, 7, 10, 11, 12, 13, 14, 15, 16, 17, 18, 19, 20]. Meanwhile, many other nonlocal nonlinear integrable equations were also introduced and studied with different space and/or time coupling[10, 21, 22, 23, 24, 25, 26, 27, 28, 29, 30, 31, 32, 33]. Indeed, solution properties in several nonlocal equations had been analyzed by the inverse scattering transform method, Darboux transformation or the bilinear method. These new systems could reproduce solution patterns which had already been discovered in their local

*Address for correspondence: Y.Chen, Shanghai Key Laboratory of Trustworthy Computing, East China Normal University, Shanghai, 200062 People’s Republic of China, e-mail: ychen@sei.ecnu.edu.cn.

counterparts. Moreover, interesting behaviors such as blowing-up(i.e., collapsing) solutions[6, 16, 25] and the existence of novel richer structures were also revealed[17, 24, 29, 30, 31]. A connection between nonlocal and local equations was discovered in [25], where it was shown that many nonlocal equations could be converted to local equations through transformations.

In this article, we study high-order solitons and their dynamics in the \mathcal{PT} -symmetric NLS equation (1) as well as the reverse-time NLS equation[10]:

$$iq_t(x, t) = q_{xx}(x, t) + 2q^2(x, t)q(x, -t), \quad (2)$$

and the reverse-space-time NLS equation[10]:

$$iq_t(x, t) = q_{xx}(x, t) + 2q^2(x, t)q(-x, -t). \quad (3)$$

Introducing the following coupled Schrödinger equations[1, 2, 5]:

$$iq_t = q_{xx} - 2q^2r, \quad (4)$$

$$ir_t = -r_{xx} + 2r^2q. \quad (5)$$

Then, equations (1)-(3) can be respectively obtained from the coupled system (4)-(5) under nonlocal reductions

$$r(x, t) = -q^*(-x, t), \quad (6)$$

$$r(x, t) = -q(x, -t), \quad (7)$$

$$r(x, t) = -q(-x, -t). \quad (8)$$

As we know, the inverse scattering transform method indicates that it is the poles of reflection coefficient (or zeros of the Riemann-Hilbert problem) that give rise to the soliton solutions. In [19], general N -solitons, which corresponds to N -simple poles in the spectral plane, are derived for nonlocal equations (1)-(3) using the inverse scattering and Riemann-Hilbert method. From this Riemann-Hilbert framework, new types of multi-solitons with novel eigenvalue configurations in the spectral plane are discovered. Therefore, as a more general case, soliton solutions correspond to multiple poles, that is, the high-order solitons can be taken into consideration for nonlocal NLS equations (1)-(3).

This kind of soliton have wide applications, it can describe a weak bound state of solitons and may appear in the study of train propagation of solitons with nearly equal velocities and amplitudes but having a particular chirp[34]. High-order soliton for several local equations, such as the Sine-Gordon, nonlinear Schrödinger, Kadomtsev-Petviashvili I and Landau-Lifshitz equations, have been investigated in several literature before[34, 35, 36, 37, 41, 42]. To the best of our knowledge, high-order soliton for the nonlocal NLS equations (1)-(3) have never been reported.

In this article, we derive the general high-order solitons in the \mathcal{PT} -symmetric, reverse-time, and reverse-space-time nonlocal NLS equations (1)-(3). These high-order solitons are reduced from the same Riemann-Hilbert solutions of the AKNS hierarchy with different symmetry relations on the “perturbed” scattering data, which consist of the “perturbed” eigenvalues as well as the corresponding eigenfunctions. Dynamics of these solitons are also explored. We show that a generic feature for high-order solitons in all the three nonlocal equations is repeated collapsing, resemble those in the (first-order) N -solitons for the nonlocal NLS equations (1)-(3). We also show that the high-order fundamental-soliton describes several travelling waves moving on different trajectories with nearly equal velocities. While the high-order multi-solitons could have more complicated wave and trajectory structures which behave very differently from the high-order fundamental-soliton. For this pattern, the corresponding eigenvalue configuration always have equal numbers of zeros with equal order in the upper and lower complex planes. Moreover, we find the high-order hybrid-pattern solitons, which corresponds to novel eigenvalue configurations, i.e., combinations between zeros of unequal order in the upper and lower complex planes. These new patterns can describe the nonlinear interaction between several types of solitons, and exhibit distinctively dynamical patterns which have not been found before.

2 High-order solitons for general coupled Schrödinger equations

To derive high-order solitons in equations (1)-(3), we need to start with the Riemann-Hilbert solutions of high-order solitons for the coupled Schrödinger equations for given scattering data. Then, imposing appropriate symmetry relations on the scattering data, the high-order solitons for each nonlocal equations can be obtained.

The coupled system (4)-(5) admits the following Lax-pair[1, 2]:

$$Y_x = -i\zeta\Lambda Y + QY, \quad (9)$$

$$Y_t = 2i\zeta^2\Lambda Y - 2\zeta QY - i\Lambda(Q_x - Q^2)Y, \quad (10)$$

where,

$$\Lambda = \text{diag}(1, -1), \quad Q(x, t) = \begin{pmatrix} 0 & q(x, t) \\ r(x, t) & 0 \end{pmatrix}. \quad (11)$$

For localized functions $q(x, t)$ and $r(x, t)$, the inverse scattering transform and the modern Riemann-Hilbert method was developed in[2, 38, 39, 40]. Following this Riemann-Hilbert treatment, N-solitons in coupled Schrödinger system can be written as ratios of determinants [3, 5] :

$$q(x, t) = 2i \frac{\begin{vmatrix} M & \bar{Y}_2^T \\ Y_1 & 0 \end{vmatrix}}{|M|}, \quad r(x, t) = -2i \frac{\begin{vmatrix} M & \bar{Y}_1^T \\ Y_2 & 0 \end{vmatrix}}{|M|}, \quad (12)$$

where, $Y = (v_1(x, t), \dots, v_N(x, t))$, $\bar{Y} = (\bar{v}_1(x, t), \dots, \bar{v}_N(x, t))$. Y_k and \bar{Y}_k represents the k -th row of matrix Y and \bar{Y} , respectively.

Here $v_k(x, t)$ and $\bar{v}_k(x, t)$ are both column vectors given by

$$v_k(x, t) = \exp[-i\zeta_k\Lambda x + 2i\zeta_k^2\Lambda t]v_{k0}, \quad (13)$$

$$\bar{v}_k(x, t) = \exp[i\bar{\zeta}_k\Lambda x - 2i\bar{\zeta}_k^2\Lambda t]\bar{v}_{k0}. \quad (14)$$

M is a $N \times N$ matrix defined as:

$$M = \left(M_{j,k}^{(N)} \right)_{1 \leq j, k \leq N}, \quad M_{j,k}^{(N)} = \frac{\bar{v}_j^T v_k}{\zeta_j - \zeta_k}, \quad 1 \leq j, k \leq N, \quad (15)$$

here $\zeta_k \in \mathbb{C}_+$ (upper half complex plane), $\bar{\zeta}_k \in \mathbb{C}_-$ (lower half complex plane), v_{k0} , \bar{v}_{k0} are constant column vectors of length two.

With this formula, the general high-order solitons can be directly obtained through a simple limiting process. For this purpose, setting N discrete spectral in the eigenfunction (13) to be:

$$\begin{aligned} \zeta_2 &= \zeta_1 + \epsilon_{1,1}, \dots, \zeta_{n_1} = \zeta_1 + \epsilon_{1,n_1-1}, \\ \zeta_{n_1+1} &= \zeta_2, \zeta_{n_1+2} = \zeta_2 + \epsilon_{2,1}, \dots, \zeta_{n_1+n_2} = \zeta_2 + \epsilon_{2,n_2-1}, \\ &\dots \\ \zeta_{N-n_r+1} &= \zeta_r, \zeta_{N-n_r+2} = \zeta_r + \epsilon_{r,1}, \dots, \zeta_N = \zeta_r + \epsilon_{r,n_r-1}. \end{aligned}$$

Similarly, setting another N discrete spectral in the adjoint eigenfunction (14) to be:

$$\begin{aligned} \bar{\zeta}_2 &= \bar{\zeta}_1 + \bar{\epsilon}_{1,1}, \dots, \bar{\zeta}_{\bar{n}_1} = \bar{\zeta}_1 + \bar{\epsilon}_{1,\bar{n}_1-1}, \\ \bar{\zeta}_{\bar{n}_1+1} &= \bar{\zeta}_2, \bar{\zeta}_{\bar{n}_1+2} = \bar{\zeta}_2 + \bar{\epsilon}_{2,1}, \dots, \bar{\zeta}_{\bar{n}_1+\bar{n}_2} = \bar{\zeta}_2 + \bar{\epsilon}_{2,\bar{n}_2-1}, \\ &\dots \\ \bar{\zeta}_{N-\bar{n}_s+1} &= \bar{\zeta}_s, \bar{\zeta}_{N-\bar{n}_s+2} = \bar{\zeta}_s + \bar{\epsilon}_{s,1}, \dots, \bar{\zeta}_N = \bar{\zeta}_s + \bar{\epsilon}_{s,\bar{n}_s-1}. \end{aligned}$$

Here, we should have $\sum_{i=1}^r n_i = \sum_{i=1}^s \bar{n}_i = N$, and $r, s \in \mathbb{Z}_+$.

Then we have the following expansions:

$$v_j(\zeta_j + \epsilon_{j,k_j}) = \sum_{k=0}^{\infty} v_j^{(k)} \epsilon_{j,k_j}^k, \quad \bar{v}_i(\bar{\zeta}_i + \bar{\epsilon}_{i,k_i}) = \sum_{k=0}^{\infty} \bar{v}_i^{(k)} \bar{\epsilon}_{i,k_i}^k,$$

$$\frac{\bar{v}_i^T(\bar{\zeta}_i + \bar{\epsilon}_{i,k_i}) v_j(\zeta_j + \epsilon_{j,k_j})}{\bar{\zeta}_i - \zeta_j + \bar{\epsilon}_{i,k_i} - \epsilon_{j,k_j}} = \sum_{l=0}^{\infty} \sum_{k=0}^{\infty} M_{i,j}^{[k,l]} \bar{\epsilon}_{i,k_i}^l \epsilon_{j,k_j}^k.$$

Therefore, applying these expansions to each matrix element in N-soliton formula (12), performing simple determinant manipulations and taking the limits of $\epsilon_{j,k_j}, \bar{\epsilon}_{i,k_i} \rightarrow 0$ ($k_j = 1, \dots, n_j - 1$, $k_i = 1, \dots, \bar{n}_i - 1$), we derive the general high-order solitons for coupled Schrödinger equations (4)-(5), which are summarized in the following theorem.

Theorem 1. *The general high-order solitons in the coupled Schrödinger equations (4)-(5) can be formulated as:*

$$q(x, t) = 2i \frac{\tau_{12}}{\tau_0}, \quad r(x, t) = -2i \frac{\tau_{21}}{\tau_0}, \quad (16)$$

where

$$\tau_0 = \det(M), \quad \tau_{kj} = \det \begin{pmatrix} M & \bar{\phi}_j^T \\ \phi_k & 0 \end{pmatrix},$$

$$M = (M_{i,j})_{1 \leq i \leq s, 1 \leq j \leq r}, \quad M_{i,j} = \left(M_{i,j}^{[k,l]} \right)_{0 \leq k \leq \bar{n}_i - 1, 0 \leq l \leq n_j - 1},$$

and

$$\phi = \left[v_1^{(0)}, \dots, v_1^{(n_1-1)}, \dots, v_r^{(0)}, \dots, v_r^{(n_r-1)} \right],$$

$$\bar{\phi} = \left[\bar{v}_1^{(0)}, \dots, \bar{v}_1^{(\bar{n}_1-1)}, \dots, \bar{v}_s^{(0)}, \dots, \bar{v}_s^{(\bar{n}_s-1)} \right].$$

Here, ϕ_k stands the k -th row in matrix ϕ , so is for $\bar{\phi}_j$.

This general soliton formula (16) has been reported in [41] (Via using dressing method) as well as in [42] (By the generalized Darboux transformation). So the proof of this theorem can be given along the lines of [41, 42].

3 Symmetry relations of “perturbed” scattering data in the nonlocal NLS equations

We first recall relevant results on symmetry relations of scattering data for the nonlocal NLS equations (1)-(3) presented in [19]. For this purpose, we denote:

$$v_{k0} = [a_k, b_k]^T, \quad \bar{v}_{k0} = [\bar{a}_k, \bar{b}_k]^T. \quad (17)$$

Next, with initial condition on the potential matrix:

$$Q_0 := Q(x) = \begin{pmatrix} 0 & q(x, 0) \\ r(x, 0) & 0 \end{pmatrix}, \quad (18)$$

here $q(x, 0), r(x, 0)$ are the initial value of functions $q(x, t)$ and $r(x, t)$ at $t = 0$.

Considering the eigenvalue problem

$$Y_x = -i\zeta \Lambda Y + Q_0 Y, \quad (19)$$

and its adjoint eigenvalue problem

$$K_x^T = i\zeta K^T \Lambda - K^T Q_0. \quad (20)$$

Therefore, by using the symmetry of potential matrix Q_0 for each nonlocal reduction (6)-(8), along with the large- x asymptotics of ζ_k 's eigenfunction $Y_k(x)$ as well as $\bar{\zeta}_k$'s eigenfunction $K_k(x)$, ref.[19] derives the connections

between each subset of scattering data $\{\zeta_k, a_k, b_k\}$ and $\{\bar{\zeta}_k, \bar{a}_k, \bar{b}_k\}$ with rigorous proof. Here, these important results can be directly used for our purpose.

In the following, we intend to show that: through a simple modification to the original scattering data, new free parameters can be introduced. In that case, we modify the existing scattering data with a perturbation, i.e.,

$$\{\zeta_k, a_k, b_k\} \mapsto \{\zeta_k(\epsilon), a_k(\epsilon), b_k(\epsilon)\}, \quad (21)$$

where $\zeta_k(\epsilon) := \zeta_k + \epsilon$, and $a_k(\epsilon)$ and $b_k(\epsilon)$ can be further defined as:

$$a_k(\epsilon) := e^{\phi_0 + \phi_1 \epsilon + \phi_2 \epsilon^2 + \dots}, \quad b_k(\epsilon) := e^{\varphi_0 + \varphi_1 \epsilon + \varphi_2 \epsilon^2 + \dots}. \quad (22)$$

Here, ϕ_k, φ_j are free complex parameters.

For the \mathcal{PT} -symmetric NLS equation (1), following the derivation of **Theorem 1** in [19] and using the large- x asymptotics of eigenfunctions, we can obtain the symmetry relations of “perturbed” scattering data (21)-(22), which are summarized as: For a pair of non-imaginary eigenvalues $(\zeta_k, \hat{\zeta}_k) \in \mathbb{C}_+$, $\hat{\zeta}_k = -\zeta_k^*$, the corresponding “perturbed” eigenvalues are defined as $(\zeta_k(\epsilon), \hat{\zeta}_k(\epsilon)) \in \mathbb{C}_+$, where $\hat{\zeta}_k(\epsilon) \equiv -\zeta_k^*(\epsilon)$. After scaling the first element $a(\epsilon)$ to 1, the “perturbed” eigenvectors $v_{k0}(\epsilon)$ and $\hat{v}_{k0}(\epsilon)$ are related as

$$\hat{v}_{k0}(\epsilon) = \sigma_1 v_{k0}^*(\epsilon), \quad v_{k0}(\epsilon) = \left[1, e^{\sum_{j=0}^{\infty} b_{kj} \epsilon^j}\right]^T, \quad b_{kj} \in \mathbb{C}. \quad (23)$$

Repeating above arguments on the adjoint eigenvalue problem, we have: for a pair of non-imaginary $(\bar{\zeta}_k, \hat{\bar{\zeta}}_k) \in \mathbb{C}_-$, $\hat{\bar{\zeta}}_k = -\bar{\zeta}_k^*$, the “perturbed” eigenvalues are defined as $(\bar{\zeta}_k(\bar{\epsilon}), \hat{\bar{\zeta}}_k(\bar{\epsilon})) \in \mathbb{C}_-$, where $\hat{\bar{\zeta}}_k(\bar{\epsilon}) \equiv -\bar{\zeta}_k^*(\bar{\epsilon})$, and the form of their eigenvectors can be similarly obtained as

$$\hat{\bar{v}}_{k0}(\bar{\epsilon}) = \sigma_1 \bar{v}_{k0}^*(\bar{\epsilon}), \quad \bar{v}_{k0}(\bar{\epsilon}) = \left[1, e^{\sum_{j=0}^{\infty} \bar{b}_{kj} \bar{\epsilon}^j}\right]^T, \quad \bar{b}_{kj} \in \mathbb{C}. \quad (24)$$

Especially, if $\zeta_k(\epsilon)$ is purely imaginary, from above definition of “perturbed” eigenvalues, we have $\hat{\zeta}_k(\epsilon) = \zeta_k(\epsilon)$. Because $-\zeta_k^* = \zeta_k$, thus, we have $\epsilon^* = -\epsilon$. In this case, their “perturbed” eigenvectors are also the same, which can be further scaled into the following form:

$$\hat{v}_{k0}(\epsilon) = v_{k0}(\epsilon) = \left[1, e^{\sum_{j=0}^{\infty} (i)^{j+1} \theta_{kj} \epsilon^j}\right]^T, \quad \theta_{kj} \in \mathbb{R}. \quad (25)$$

Similarly, when $\bar{\zeta}_k(\bar{\epsilon})$ is also purely imaginary, its eigenvector is of the form:

$$\hat{\bar{v}}_{k0}(\bar{\epsilon}) = \bar{v}_{k0}(\bar{\epsilon}) = \left[1, e^{\sum_{j=0}^{\infty} (i)^{j+1} \bar{\theta}_{kj} \bar{\epsilon}^j}\right]^T, \quad \bar{\theta}_{kj} \in \mathbb{R}. \quad (26)$$

Next, for the reverse-time NLS equation (2). Following the derivation of **Theorem 2** in [19] as well as the above analysis, we can also derive the symmetry relations of its “perturbed” scattering data, which is represented as: For a pair of discrete eigenvalues $(\zeta_k, \bar{\zeta}_k)$, where $\zeta_k \in \mathbb{C}_+$ and $\bar{\zeta}_k = -\zeta_k \in \mathbb{C}_-$. The “perturbed” eigenvalues are defined as $(\zeta_k(\epsilon), \bar{\zeta}_k(\bar{\epsilon}))$, where $\zeta_k(\epsilon) \in \mathbb{C}_+$, and $\bar{\zeta}_k(\bar{\epsilon}) \equiv -\zeta_k(-\bar{\epsilon}) \in \mathbb{C}_-$. Then we scale the “perturbed” eigenvectors $v_{k0}(\epsilon)$ and $\bar{v}_{k0}(\bar{\epsilon})$ with their first elements become 1, and they are related as:

$$v_{k0}(\epsilon) = [1, e^{\sum_{j=0}^{\infty} b_{k,j} \epsilon^j}]^T, \quad \bar{v}_{k0} = v_{k0}(-\bar{\epsilon}), \quad b_{kj} \in \mathbb{C}. \quad (27)$$

where b_k is an arbitrary complex parameter.

However, for the reverse-space-time NLS equation (3), according to the symmetry relations on the scattering data given by **Theorem 3** in [19], i.e., the eigenvalues ζ_k can be anywhere in \mathbb{C}_+ and $\bar{\zeta}_k$ can be anywhere in \mathbb{C}_- . And the corresponding eigenvectors must be of the forms

$$v_{k0} = [1, \omega_k]^T, \quad \omega_k = \pm 1; \quad \bar{v}_{k0} = [1, \bar{\omega}_k]^T, \quad \bar{\omega}_k = \pm 1. \quad (28)$$

We find that all the parameters in the “perturbed” scattering data can be eliminated in the “perturbed” eigenvectors. Thus, no more parameters can be introduced in (28) so that we have $v_{k0}(\epsilon) = v_{k0}$, $\bar{v}_{k0}(\bar{\epsilon}) = \bar{v}_{k0}$.

Therefore, utilizing the above symmetry relations on the “perturbed” scattering data in the high-order Riemann-Hilbert solution (16), we will construct high-order solitons for nonlocal NLS equations (1)-(3) in the sections below.

4 Dynamics of high-order solitons in the \mathcal{PT} -symmetric nonlocal NLS equation

To derive the N -th order solitons in the \mathcal{PT} -symmetric NLS equation (1), we just need to apply corresponding symmetry relations of the scattering data to the general soliton formula (16). Then we investigate solution dynamics in the high-order fundamental (one)-soliton as well as the high-order multi-solitons.

4.1 High-order fundamental-soliton

Firstly, we consider the second-order fundamental-soliton, which corresponds to a single pair of purely imaginary eigenvalues (zero of multiplicity two) $\zeta_1 = i\eta_1 \in i\mathbb{R}_+$, and $\bar{\zeta}_1 = i\bar{\eta}_1 \in i\mathbb{R}_-$, where $\eta_1 > 0$ and $\bar{\eta}_1 < 0$. In this case, symmetry relations on the perturbed eigenfunctions are given by (25)-(26), i.e., $v_{10}(\epsilon) = [1, e^{i\theta_{10}-\theta_{11}\epsilon}]^T$, and $\bar{v}_{10}(\bar{\epsilon}) = [1, e^{i\bar{\theta}_{10}-\bar{\theta}_{11}\bar{\epsilon}}]^T$, where $\theta_{10}, \theta_{11}, \bar{\theta}_{10}, \bar{\theta}_{11}$ are real constants. Substituting these expressions into formula (16) with $N = n_1 = \bar{n}_1 = 2$, we obtain the analytic expression for the second-order fundamental soliton of equation (1):

$$q(x, t) = \frac{2(\bar{\eta}_1 - \eta_1) \left[\mathcal{G}(x, t) e^{2\bar{\eta}_1 x - 4i\bar{\eta}_1^2 t + i\bar{\theta}_{10}} + \bar{\mathcal{G}}(x, t) e^{2\eta_1 x - 4i\eta_1^2 t - i\theta_{10}} \right]}{4 \cosh^2 \left[(\eta_1 - \bar{\eta}_1)x - 2i(\eta_1^2 - \bar{\eta}_1^2)t - \frac{i}{2}(\theta_{10} + \bar{\theta}_{10}) \right] + \mathcal{F}(x, t)}, \quad (29)$$

where $\mathcal{F}(x, t) = -(\mathcal{G} + 2)(\bar{\mathcal{G}} + 2)$, with

$$\mathcal{G}(x, t) = (\bar{\eta}_1 - \eta_1)(2x - 8i\eta_1 t + i\theta_{11}) - 2, \quad (30)$$

$$\bar{\mathcal{G}}(x, t) = (\eta_1 - \bar{\eta}_1)(2x - 8i\bar{\eta}_1 t - i\bar{\theta}_{11}) - 2. \quad (31)$$

This kind of soliton, which combines exponential functions with algebraic polynomials, has never been reported before in the nonlocal NLS equation (1). It contains six real parameters: $\eta_1, \bar{\eta}_1, \theta_{10}, \bar{\theta}_{10}, \theta_{11}$ and $\bar{\theta}_{11}$. The motion trajectory for this solution can be approximatively described by the following two curves

$$\Sigma_{\pm} : 2(\bar{\eta}_1 - \eta_1)x \pm \ln |\mathcal{F}(x, t)| = 0. \quad (|\mathcal{F}(x, t)| \neq 0) \quad (32)$$

In this case, two solitons moving along the center trajectories Σ_+ and Σ_- . When $|x| \rightarrow \pm\infty$, the amplitude $|q|$ of the solution decays exponentially to zero. However, with the development of time, a simple asymptotic analysis with estimation on the leading-order terms shows that: when soliton (29) is moving on Σ_+ or Σ_- , its amplitudes $|q|$ can approximatively vary as:

$$|q(x, t)| \sim \frac{2|\eta_1 - \bar{\eta}_1| e^{(\eta_1 + \bar{\eta}_1)z(x, t)}}{|e^{\pm 2i\gamma t - i\tau_0 \pm i(\theta_{10} + \bar{\theta}_{10})} + 1|}, \quad t \sim \pm\infty, \quad (33)$$

where $z(x, t) = \frac{\ln |\mathcal{F}(x, t)|}{\pm 2(\eta_1 - \bar{\eta}_1)}$, $\gamma = 2(\bar{\eta}_1^2 - \eta_1^2)$, $\tau_0 = \text{Arg}[\mathcal{F}(x, t)] + 2k\pi$, ($k \in \mathbb{Z}$), the positive and negative sign in (33) respectively corresponds to Σ_+ and Σ_- . (It should be noted that estimation (33) is valid only when $|t| \gg \max\{|\theta_{11}|, |\bar{\theta}_{11}|\}$. Before this, the amplitudes $|q|$ of solution are unequal when soliton moves on each curve, depending on the value of parameter θ_{11} and $\bar{\theta}_{11}$.)

In the case when $\eta_1 = -\bar{\eta}_1$, solution (29) will be nonsingular or collapsing at certain locations, depending on the values of these parameters. Specifically,

(1). If $\theta_{11} = \bar{\theta}_{11}$, as long as $\theta_{10} + \bar{\theta}_{10} \neq (2k + 1)\pi$ for any integer k , this soliton will be nonsingular.

(2). If $\theta_{11} \neq \bar{\theta}_{11}$, we first define three multivariate functions, these are $c_0 \equiv \frac{\sin(\theta_{10} + \bar{\theta}_{10})}{\eta_1(\theta_{11} - \bar{\theta}_{11})}$, $\Delta_1 \equiv \frac{(\theta_{11} - \bar{\theta}_{11})^2}{4} - \frac{1 + \cos(\theta_{10} - \bar{\theta}_{10})}{2\eta_1^2}$ and $\Delta_2 \equiv -4x_c^2 + \frac{(\theta_{11} - \bar{\theta}_{11})^2}{4} - \frac{1 + \cosh(4\eta_1 x_c) \cos(\theta_{10} - \bar{\theta}_{10})}{2\eta_1^2}$, which contain all the parameters. Then, solution (29) will not blow up only when c_0 , Δ_1 and Δ_2 satisfy one of the following two critical conditions:

$$(a). \text{ For any } \theta_{10} + \bar{\theta}_{10} \neq (2k + 1)\pi, c_0 \notin (0, 1), \text{ and } \Delta_1 < 0. \quad (34)$$

$$(b). c_0 \in (0, 1), \text{ and } \Delta_1, \Delta_2 < 0. \quad (35)$$

Otherwise, when $\Delta_1 \geq 0$ in condition (a), there will be two(or one) singular points locating at $x = 0$, $t = \frac{\pm\sqrt{\Delta_1}}{8\eta_1} + t_0$, where $t_0 = \frac{\theta_{11}-\bar{\theta}_{11}}{16\eta_1}$. Or, when $\Delta_2 \geq 0$ with $c_0 \in (0, 1)$ in (b), there would also have two(or one) singular points locating at $x = x_c$, $t = \frac{\pm\sqrt{\Delta_2}}{8\eta_1} + t_0$. Here x_c admits a special transcendental equation $\frac{4\eta_1 x_c}{\sinh(4\eta_1 x_c)} = c_0$, which can be solved numerically for this given c_0 .

Moreover, for all the nonsingular solution, $|q(x, t)|$ reaches its peak amplitude at $x = 0$, $t = t_0$ with the value attained as $\left| \frac{8\eta_1 [\eta_1 (\theta_{11} - \bar{\theta}_{11}) \sin(\phi_0) - 2 \cos(\phi_0)]}{4 \cos^2(\phi_0) - \eta_1^2 (\theta_{11} - \theta_{11})^2} \right|$, where $\phi_0 = \frac{\theta_{10} + \bar{\theta}_{10}}{2}$. When $t \rightarrow \pm\infty$, according to a logarithmic law for large values of $|t|$, two solitons moving along Σ_+ and Σ_- with almost equal velocities and amplitudes, and peak amplitude does not exceed $\left| \frac{4\eta_1}{1 + e^{i(\theta_1 + \bar{\theta}_1)}} \right|$. To demonstrate, we choose the following parameters:

$$\eta_1 = 0.5, \theta_{10} = \pi/4, \bar{\theta}_{10} = \pi/6, \theta_{11} = 0.25, \bar{\theta}_{11} = 0.5. \quad (36)$$

Propagation of this high-order soliton is displayed in Fig.1.

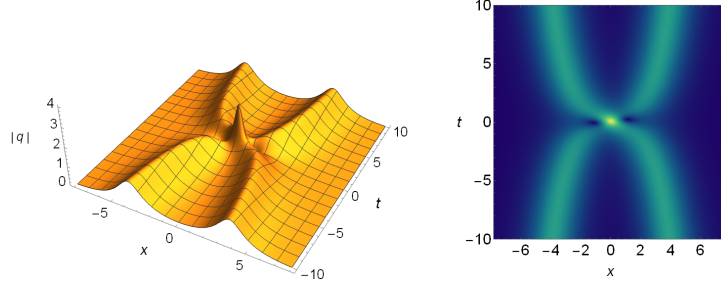


Figure 1: Left panel is the second-order one-soliton (29) with parameters (36). Right panel is the corresponding density plot.

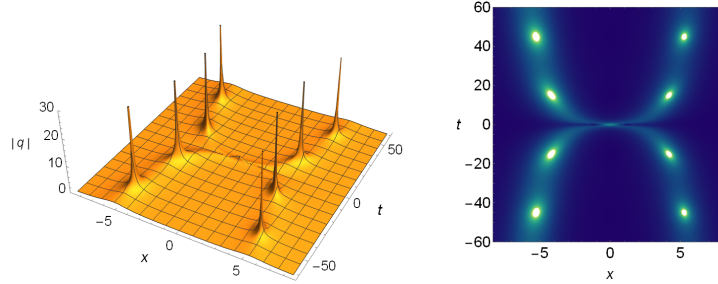


Figure 2: Left panel is the 2nd-order one-soliton (29) in eq.(1) with parameters (37). Right panel is the corresponding density plot.(Here, the bright spots shown on the density plot represent the location of singularity.)

It is shown that two solitons are slowly moving in the spatial orientation. This is quite different from the dynamics of fundamental soliton in [19], where the soliton can not move in space. The peak amplitude of $|q(x, t)|$ reaches about 2.65834 at the location $(0, 0.09375)$. Moreover, with the evolution of time, they keep almost identical value of maximum amplitudes, which is no larger than about 1.26047.

In a more general case, where $\eta_1 \neq -\bar{\eta}_1$, an important feature for this high-order soliton is the repeatedly collapsing along two trajectories. This can be clarified from the large-time estimation (33). Actually, when $|t|$ becomes very large, a direct calculation shows that $\lim_{|t| \rightarrow \infty} \text{Arg} [\mathcal{F}(x, t)] = \pi$. Thus, one can repeatedly choose large time point t_c s.t. $\cos(2\gamma t_c \mp \tau_0 + (\theta_{10} + \bar{\theta}_{10})) = -1$. This implies the existence of singularities for the solution at large time.

Moreover, due to the impact of algebraic polynomial terms, the collapsing interval for this high-order soliton is no more a fixed value. Instead, this so-called “period” is slightly varying over time. Besides, amplitudes of solution $|q|$ are unequal when soliton moves on each path, depending on the sign of $\eta_1 + \bar{\eta}_1$. To illustrate, we choose parameters as

$$\eta_1 = 0.50, \bar{\eta}_1 = -0.55, \theta_{10} = \bar{\theta}_{10} = 0, \theta_{11} = \bar{\theta}_{11} = 0. \quad (37)$$

Graphs of corresponding second-order fundamental-soliton are shown in Fig.2. Through simple numerical calculation and approximate estimation, the first singularities quartet for this soliton is obtained, which locates approximately at $(\pm x_c, \pm t_c)$ with $x_c \approx 3.9999$, $t_c \approx 15.0169$, and the first time interval between two successive singularities $\pm t_c$ is 30.0338. Afterwards, the second singularities quartet approximately appears at $(\pm \tilde{x}_c, \pm \tilde{t}_c)$ with $\tilde{x}_c \approx 5.0369$, $\tilde{t}_c \approx 44.9041$. So the second time interval between \tilde{t}_c and t_c is about 29.9232.

Generally, the N -th order fundamental-soliton solution can be obtained in the same way by choosing $n_1 = \bar{n}_1 = N$ in formula (16), and the dynamics of N -wave motion on N different asymptote trajectories can be expected.

4.2 High-order multi-solitons

Now, we consider the high-order multi-solitons for the \mathcal{PT} -symmetric NLS equation. From the symmetries of scattering data, the eigenvalues in the upper and lower halves of the complex plane are completely independent. This allows for novel eigenvalue configurations, which gives rise to new types of high-order solitons with interesting dynamical patterns. These results can be divided into the following two cases in principle:

4.2.1 The normal pattern: Square-matrix blocks.

For the most normal pattern, each block $(M_{i,j}^{[k,l]})_{0 \leq k \leq \bar{n}_i - 1, 0 \leq l \leq n_j - 1}$ of $(M_{i,j})_{1 \leq i \leq s, 1 \leq j \leq r}$ in formula(16) is an square matrix. In this case, one has to take the same index $s = r = m$ with $n_k = \bar{n}_k = n$ ($k = 1, 2, \dots, m$) and $N = n \times m$ in (16). This yields the normal N -th order m -solitons.

For example, we consider the second-order two-soliton. Especially, choosing a pair of non-purely-imaginary eigenvalues: $\zeta_1, \zeta_2 \in \{\mathbb{C}_+ \setminus i\mathbb{R}_+\}$ with $\zeta_2 = -\zeta_1^*$, which belongs to the second type two-solitons for eq.(1) discussed in [19]. Thus, from above results (23)-(24), their perturbed eigenvalues and eigenvectors are related as

$$\zeta_2(\epsilon) = -\zeta_1^*(\epsilon), \quad v_{20}(\epsilon) = \sigma_1 v_{10}^*(\epsilon), \quad v_{10}(\epsilon) = [1, e^{b_{10} + b_{11}\epsilon}]^T,$$

where b_{10}, b_{11} are complex constants.

Similarly, for a pair of non-purely-imaginary eigenvalues $\bar{\zeta}_1, \bar{\zeta}_2 \in \{\mathbb{C}_- \setminus i\mathbb{R}_-\}$, with $\bar{\zeta}_2 = -\bar{\zeta}_1^*$, their perturbed eigenvalues and eigenfunctions are related as

$$\bar{\zeta}_2(\bar{\epsilon}) = -\bar{\zeta}_1^*(\bar{\epsilon}), \quad \bar{v}_{20}(\bar{\epsilon}) = \sigma_1 \bar{v}_{10}^*(\bar{\epsilon}), \quad \bar{v}_{10}(\bar{\epsilon}) = [1, e^{\bar{b}_{10} + \bar{b}_{11}\bar{\epsilon}}]^T,$$

where $\bar{b}_{10}, \bar{b}_{11}$ are complex constants. Substituting these data into (16) with $N = 4$, $n_1 = n_2 = 2$ and $\bar{n}_1 = \bar{n}_2 = 2$. Then it is found the corresponding solution can be nonsingular or repeatedly collapse in pairs at spatial locations. In addition, they can move in four opposite directions and exhibit more complex wave-front structures.

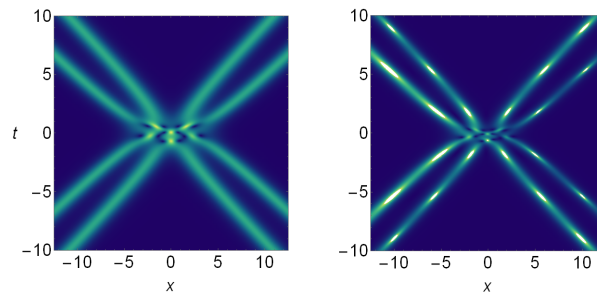


Figure 3: (a) is the second-order two-solitons with parameters (38)-(39). (b) shows the second-order two-solitons with parameters (40)-(41).

To demonstrate their dynamics, we choose two sets of parameters:

$$\zeta_1 = -\zeta_2^* = 0.3 + 0.8i, \bar{\zeta}_1 = -\bar{\zeta}_2^* = 0.3 - 0.8i, \quad (38)$$

$$e^{b_{10}} = 1 + 0.2i, e^{\bar{b}_{10}} = 1 - 0.1i, e^{b_{11}} = 0.2, e^{\bar{b}_{11}} = 0.25. \quad (39)$$

$$\zeta_1 = -\zeta_2^* = 0.3 + i, \bar{\zeta}_1 = -\bar{\zeta}_2^* = 0.3 - 1.2i, \quad (40)$$

$$e^{b_{10}} = 1 + i, e^{\bar{b}_{10}} = 1 - i, e^{b_{11}} = 1, e^{\bar{b}_{11}} = 1. \quad (41)$$

Parameter (38)-(39) generates a nonsingular solution which is plotted in the left panel of Fig.3, while the right panel in Fig.3 exhibits the blowing-up solution derived from parameter set (40)-(41). Especially, if the real parts of eigenvalues ζ_k and $\bar{\zeta}_k$ are not equal, the amplitudes of moving waves decreases or increases exponentially with time.

4.2.2 The hybrid pattern: Combination of different block types.

Secondly, we consider a more general case, where the blocks (sub-matrices) are not required to be square matrices. Instead, different types of blocks can be combined together through formula (16). Specifically, defining two index sets I_1 and I_2 for the block matrix: $I_1 = \{n_1, \dots, n_r\}$, $I_2 = \{\bar{n}_1, \dots, \bar{n}_s\}$. From above discussion we know that I_1 and I_2 are mutually independent. By virtue of this fact, novel patterns of solitons can be achieved by taking different index values. These interesting hybrid patterns have not been reported before and can describe the interactions between several one- or multi-solitons with unequal orders.

Taking $N = 2$ in formula (16), then index sets have three kinds of combinations (Regardless of other equivalent cases): (a). $I_1 = I_2 = \{1, 1\}$; (b). $I_1 = I_2 = \{2\}$; (c). $I_1 = \{1, 1\}$, $I_2 = \{2\}$. The first two combinations are the normal case, which corresponding to the two-soliton and second-order fundamental-soliton. For the last one, two simple zeros which are symmetric about the imaginary axis locates in \mathbb{C}_+ and one zero (multiplicity two) locates in \mathbb{C}_- . This interesting configuration of eigenvalues corresponds to a special “two-soliton” solution. Such an example is shown in Fig.4 with parameters:

$$\zeta_1 = -\zeta_2^* = 0.1 + 0.5i, \bar{\zeta}_1 = -0.25i, b_{10} = 0, \bar{\theta}_{10} = 0, \bar{\theta}_{11} = 0.2. \quad (42)$$

This soliton describes two waves traveling in opposite directions as they repeatedly collapsing over time. Remarkably, their motion trajectory is no longer straight line but on certain curves, which is different from the normal two-soliton. In addition, the amplitudes $|q|$ of two travelling waves are growing or decreasing exponentially with time, just along the directions of motion.

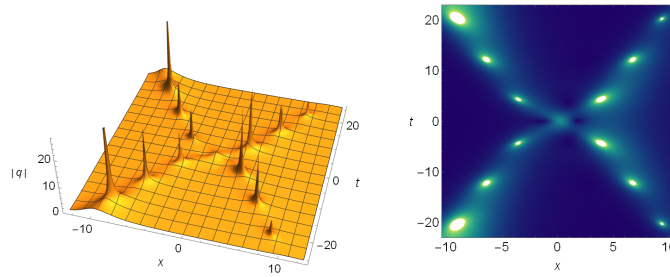


Figure 4: Left panel is a hybrid solution with parameters (42). Right panel is the corresponding density plot. (Here, the collapsing points are shown by the white bright spots, when they are amplifying or shrinking along the line, it means the solutions' amplitudes are increasing or decreasing correspondingly.)

Next, when $N = 3$, the corresponding block sets have six combinations: (a). $I_1 = I_2 = \{1, 1, 1\}$; (b). $I_1 = \{1, 1, 1\}$, $I_2 = \{1, 2\}$; (c). $I_1 = \{1, 1, 1\}$, $I_2 = \{3\}$; (d). $I_1 = \{1, 2\}$, $I_2 = \{1, 2\}$; (e). $I_1 = \{1, 2\}$, $I_2 = \{3\}$; (f). $I_1 = I_2 = \{3\}$. These sets can feature the interactions of several types of one- or multi-solitons with certain orders, except for the normal case (a) and (f).

Specifically, if we consider combination (b), there will be three simple pole in the upper half plane and one double-pole with one simple pole in the lower half plane. This eigenvalue configuration can also bring new hybrid

patterns, which feathers nonlinear superposition between a special “two-soliton” and a fundamental one-soliton. Using parameter values

$$\zeta_1 = -\zeta_2^* = 0.1 + 0.6i, \zeta_3 = 0.5i, \bar{\zeta}_1 = -0.7i, \bar{\zeta}_2 = -0.25i, \quad (43)$$

$$b_{10} = 0, \theta_{30} = \bar{\theta}_{10} = \bar{\theta}_{20} = \bar{\theta}_{21} = 0. \quad (44)$$

The associated solution is plotted in Fig.5. This soliton feathers two waves travelling in two opposite curves, plus another stationary wave (fundamental soliton) at $x = 0$, while they both collapse repeatedly along the directions. Moreover, the amplitudes of the moving waves are changing with time as well.

Consider combination (d) as another example. In this case, there is one simple pole and one double-pole in the upper half plane as well as the lower half plane. This eigenvalue configuration could create a new type of hybrid soliton which differs from other patterns. To illustrate its dynamics, we choose parameters

$$\zeta_1 = \bar{\zeta}_1^* = 0.25i, \zeta_2 = \bar{\zeta}_2^* = 0.5i, \theta_{10} = -\bar{\theta}_{20} = -\pi/6, \quad (45)$$

$$\bar{\theta}_{10} = -\theta_{20} = \pi/4, \theta_{21} = 1, \bar{\theta}_{21} = 0.5. \quad (46)$$

Corresponding graph for this solution is presented in Fig.5, which feathers the nonlinear interaction between the second-order one-soliton and a fundamental soliton.

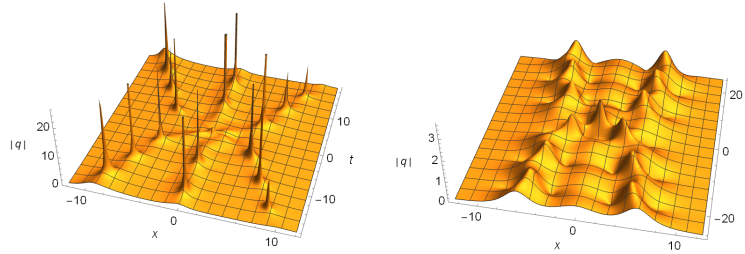


Figure 5: Left panel is a hybrid solution with parameters (45). Right panel shows a hybrid solution with parameters (43)-(44).

This soliton does not collapse and the interesting periodic phenomenon can be seen. For the rest of the combinations, we can still utilize formula (16) to generate other hybrid patterns of solitons.

Therefore, as we could see, the hybrid pattern solitons exhibit several new types of dynamics which have not been observed before. Similarly, the higher order multi-hybrid solitons can be also investigated in this way and the additional novel phenomenon can be expected.

5 Dynamics of high-order solitons in the reverse-time NLS equation

To derive N -th order solitons for the reverse-time NLS equation (2), we need to impose corresponding symmetry relations of “perturbed” discrete scattering data in the general soliton formula (16). Normally, for a pair of discrete eigenvalues $(\zeta_k, \bar{\zeta}_k)$, where $\zeta_k \in \mathbb{C}_+$ and $\bar{\zeta}_k = -\zeta_k \in \mathbb{C}_-$. From conclusion (27) in section 3, we get the corresponding “perturbed” eigenvectors

$$v_{k0}(\epsilon) = [1, e^{\sum_{j=0}^{N-1} b_{k,j} \epsilon^j}]^T, \bar{v}_{k0} = v_{k0}(-\bar{\epsilon}), b_{kj} \in \mathbb{C}. \quad (47)$$

Hence, the N -th order m -solitons have $m(N+1)$ free complex constants, $\{\zeta_k, b_{k,j}, 1 \leq k \leq m, 0 \leq j \leq N-1\}$.

The second-order fundamental-soliton is obtained when we set $N = 2, m = 1$ with $n_1 = \bar{n}_1 = 2$ in (16), and the analytical expression is:

$$q(x, t) = \frac{8\zeta_1 e^{4i\zeta_1^2 t} [e^{-2i\zeta_1 x - \ln b_{10}} f_1(x, t) + e^{2i\zeta_1 x + \ln b_{10}} \bar{f}_1(x, t)]}{4 \cosh^2(2i\zeta_1 x + \ln b_{10}) + f_0(x, t)}. \quad (48)$$

where $f_0(x, t) = 4(f_1(x, t) + i)(\bar{f}_1(x, t) + i)$, and

$$f_1(x, t) = \zeta_1(2x + 8\zeta_1 t - ib_{11}b_{10}^{-1}) - i, \quad \bar{f}_1(x, t) = \zeta_1(-2x + 8\zeta_1 t + ib_{11}b_{10}^{-1}) - i.$$

Although the fundamental-soliton in eq.(2) are found to be stationary[19]. For this second-order fundamental-soliton, two solitons moving along the path

$$\Sigma_{\pm} : 2\text{Im}(\zeta_1)x \pm \frac{1}{2} \ln |f_0(x, t)| - \ln |b_1| = 0 \quad (49)$$

with almost the same velocity. As $t \rightarrow \pm\infty$, the amplitudes $|q|$ changes as

$$|q(x, t)| \sim \frac{8|\zeta_1|e^{-4\text{Im}(\eta_1^2)t}}{|e^{\pm 2i\gamma x - i\tau_0 \pm 2i \arg(b_{10})} + 1|}, \quad (50)$$

where $\gamma = 2\text{Re}(\zeta_1)$, $\tau_0 = \text{Arg}[f_0(x, t)] + 2k\pi$, ($k \in \mathbb{Z}$).

This soliton would also collapse at certain locations, but not repeatedly collapse with time. Under a suitable choice of parameters, this high-order soliton can be non-collapsing. The amplitudes of two moving waves grows or decays exponentially when $\zeta_1 \in \{\mathbb{C}_+ \setminus i\mathbb{R}_+\}$, and it would decay/grow when ζ_1 is in the first/second quadrant of the complex plane. As concrete examples, graphs of these solitons are illustrated in Fig.6 with two sets of parameters.

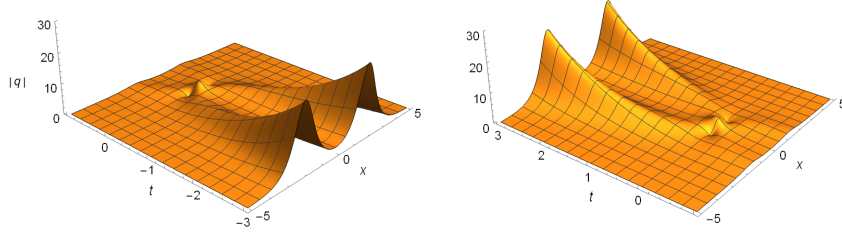


Figure 6: The second-order one-soliton (48) with parameters: (Left panel) $\zeta_1 = 0.1 + i$, $e^{b_{10}} = 1 + 0.1i$, $e^{b_{11}} = 1$. (Right panel). $\zeta_1 = -0.1 + i$, $e^{b_{10}} = e^{b_{11}} = 1$.

Normally, the N -th order fundamental-soliton could exhibit analogical features with the second-order fundamental-soliton. There will be N different asymptote trajectories with N waves moving along them in the nearly same velocities. For instance, a decaying third-order one-soliton is displayed in Fig.7. Moreover, the high-order multi-solitons could exhibit quite different dynamics. For example, the second-order two-solitons move in four opposite directions when ζ_1, ζ_2 are not both purely imaginary, and the repeated collapsing and “four-way” motion can be observed. Such an high-order two-solitons solution is shown in Fig.7, which can not be seen as a simple nonlinear superposition between two second-order fundamental-soliton.

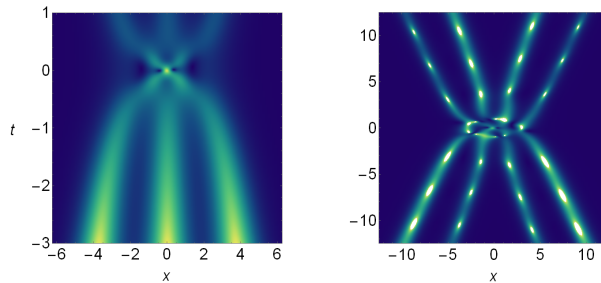


Figure 7: (Left panel). Density plot for the third-order soliton with parameters: $\zeta_1 = 0.05 + i$, $e^{b_{10}} = 1$, $e^{b_{11}} = 0.1 + 0.1i$. (Right panel). Density plot for the second-order two-solitons with parameters: $\zeta_1 = 0.2 + i$, $\zeta_2 = -0.1 + 1.2i$, $e^{b_{10}} = 1 + 0.5i$, $e^{b_{20}} = 1$, $e^{b_{11}} = e^{b_{21}} = 1$.

6 Dynamics of high-order solitons in the reverse-space-time NLS equation

To derive the N -th order solitons in the reverse-space-time NLS equation (3), we impose symmetry relations of discrete scattering data (28) in the general soliton formula (16). In this case, the normal N -th order m -solitons have $2m$ free complex constants, $\{\zeta_k, \bar{\zeta}_k, 1 \leq k \leq m\}$, where $\zeta_k \in \mathbb{C}_+$, and $\bar{\zeta}_k \in \mathbb{C}_-$.

For the second-order fundamental soliton, we choose $m = 1$ with $N = n_1 = \bar{n}_1 = 2$. So the analytic expression for this solution is

$$q(x, t) = \frac{4\bar{\omega}_1 (\zeta_1 - \bar{\zeta}_1) \left[\omega_1 \bar{\omega}_1 e^{-2i(\bar{\zeta}_1 x - 2\bar{\zeta}_1^2 t)} f_1(x, t) + e^{-2i(\zeta_1 x - 2\zeta_1^2 t)} \bar{f}_1(x, t) \right]}{e^{2i(\bar{\zeta}_1 - \zeta_1)x + 4i(\zeta_1^2 - \bar{\zeta}_1^2)t} + e^{-2i(\bar{\zeta}_1 - \zeta_1)x - 4i(\zeta_1^2 - \bar{\zeta}_1^2)t} + \omega_1 \bar{\omega}_1 f_0(x, t)}, \quad (51)$$

where $f_0(x, t) = 4(f_1 + i)(\bar{f}_1 + i) + 2$, and

$$f_1(x, t) = (\bar{\zeta}_1 - \zeta_1)(x - 4\zeta_1 t) - i, \quad \bar{f}_1(x, t) = (\zeta_1 - \bar{\zeta}_1)(x - 4\bar{\zeta}_1 t) - i,$$

It is found that the above high-order fundamental-soliton (51) has two gradually paralleled center trajectories, which approximatively locate at following two curves:

$$\Sigma_{\pm} : \operatorname{Im}(\bar{\zeta}_1 - \zeta_1)x - 2\operatorname{Im}(\bar{\zeta}_1^2 - \zeta_1^2)t \pm \frac{1}{2} \ln[|f_0 - 2|] = 0. \quad (52)$$

Moreover, regardless of the effect brought by the logarithmic part as $t \rightarrow \pm\infty$, two solitons moving separately along Σ_{\pm} each curve in a nearly same velocity, which is approximate to:

$$V \approx V_c := 2\operatorname{Im}(\bar{\zeta}_1^2 - \zeta_1^2) / \operatorname{Im}(\bar{\zeta}_1 - \zeta_1),$$

and the solution's amplitudes $|q|$ would approximately changes as:

$$|q(t)| \sim 2|\zeta_1 - \bar{\zeta}_1| \frac{e^{\beta t \pm \delta_0}}{|e^{\pm 2i\gamma t - i\tau_0} + \omega_1 \bar{\omega}_1|}, \quad t \sim \pm\infty, \quad (53)$$

where,

$$\begin{aligned} \beta &= -2V_c \operatorname{Im}(\bar{\zeta}_1) - 4\operatorname{Im}(\bar{\zeta}_1^2), \quad \gamma = V_c \operatorname{Re}(\zeta_1 - \bar{\zeta}_1) - 2\operatorname{Re}(\zeta_1^2 - \bar{\zeta}_1^2). \\ \delta_0 &= -\operatorname{Im}(\zeta_1 + \bar{\zeta}_1) \ln \sqrt{|f_0 - 2|} / \operatorname{Im}(\bar{\zeta}_1 - \zeta_1), \end{aligned}$$

with $\tau_0 = \operatorname{Arg}[f_0(x, t) - 2] + 2k\pi$, ($k \in \mathbb{Z}$).

As can be seen from this estimation, the amplitude of soliton is growing or decaying exponentially along Σ_{\pm} at the rate of $e^{\beta t \pm \delta_0}$, which depends mainly on the value of β (except for $\operatorname{Re}(\zeta_1) = \operatorname{Re}(\bar{\zeta}_1)$, where $\beta = 0$). These are also some difference in the amplitudes when $q(x, t)$ moves on different trajectories, depending on the sign of δ_0 . Especially, if $\delta_0 = 0$, both of them will keep the same amplitude.

Another interesting feature for this high-order fundamental soliton is the repeatedly collapsing phenomenon. And the blowing-up interval T_c for this solution admits a ‘‘perturbative’’ varying period, which can be roughly estimated as: $T_c = \pi/|\gamma| + \Delta(t)$, where $\Delta(t)$ is a time-dependent small error term. Regardless of minor changes in the arguments $\tau_0(t)$, the approximatively value of $\Delta(t)$ is attained as $\Delta(t) \approx [\bar{\tau}_0(t_c + \pi/|\gamma|) - \tau_0(t_c)] / 2\gamma$, where t_c is the time coordinate for an initial singularity. Examples are given for two sets of parameters:

$$\zeta_1 = -0.3 + 0.9i, \quad \bar{\zeta}_1 = -0.28 - 0.6i, \quad \omega_1 = \bar{\omega}_1 = 1, \quad (54)$$

$$\zeta_1 = 0.35 + 0.9i, \quad \bar{\zeta}_1 = 0.325 - 0.6i, \quad \omega_1 = -\bar{\omega}_1 = 1. \quad (55)$$

Graphs of the two fundamental solitons are displayed respectively in Fig.8. Apparently, both of these two solitons collapse repeatedly with time. In the former solution, the soliton moves at velocity about $V_c \approx -1.168$ (to the

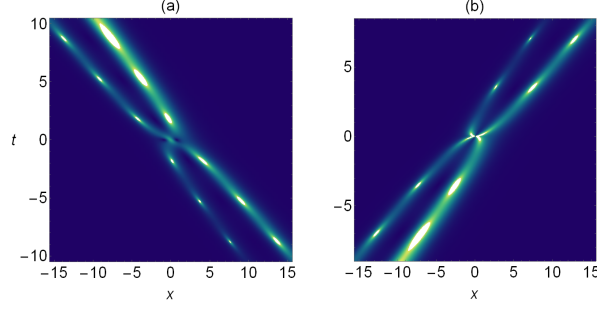


Figure 8: Two second-order one-solitons (51) in the reverse-space-time NLS equation (3). The parameters for the density plot (a). and (b). are given by Eqs. (54) and (55) respectively.

left). The amplitude $|q|$ exponentially increases along the curve Σ_{\pm} at the rate of $e^{\beta t}$ with $\beta \approx 0.0576$. In the latter solution, the soliton moves at velocity $V_c \approx 1.36$ (to the right), while $|q|$ decreases exponentially along Σ_{\pm} at the rate of $e^{\beta t}$ with $\beta \approx -0.072$.

For the the high-order multi-solitons, because the eigenvalues $\zeta_k \in \mathbb{C}_+$ and $\bar{\zeta}_k \in \mathbb{C}_-$ are totally independent, eigenvalues can be also arranged in several different configurations, which give rise to new types of solitons for the reverse-space-time NLS equation (3). For instance, with symmetry (28) on the eigenvectors, if we take $N = 2$ with $I_1 = \{1, 1\}$ and $I_2 = \{2\}$ in formula (16), certain choice of parameters can produce a high-order “two-soliton”. Choosing $N = 4$ with $I_1 = I_2 = \{2, 2\}$, we can derive a nonlinear superposition between two different second-order one-soliton solutions (This solution can be also regarded as a second-order two-soliton). Graphs of these solitons are very similar to those displayed in Fig.3 and Fig.4, so their novel dynamic behaviors can be expected.

7 Summary and discussion

In summary, we have derived general high-order solitons in the \mathcal{PT} -symmetric, reverse-time, and reverse-space-time nonlocal NLS equations (1)-(3) by using a Riemann-Hilbert treatment. We have shown that through the symmetry relations on the “perturbed” scattering data in each equation, the high-order solitons can be separately reduced from the Riemann-Hilbert solutions of the AKNS hierarchy. At the same time, novel solution behaviours in these nonlocal equations have been further discussed. We have found that the high-order fundamental-soliton is always moving on several trajectories in nearly equal velocities, while the high-order multi-solitons could have more complicated wave and trajectory structures. In all these nonlocal equations, a generic character in their high-order solitons is repeated collapsing. Moreover, new types of high-order hybrid-pattern solitons are discovered, which can describe a nonlinear superposition between several types of solitons. Our findings reveal the novel and rich structures for high-order solitons in the nonlocal NLS equations (1)-(3), and they could intrigue further investigations on solitons in the other nonlocal integrable equations.

In addition, it should be noted that by utilizing new symmetry properties of scattering data in these nonlocal equations, some open questions left over in previous Riemann-Hilbert derivations of solitons have been resolved in [19]. That is, when the numbers of eigenvalues (or, known as zeros of the Riemann-Hilbert problem) in the upper and lower complex planes, counting multiplicity, are not equal to each other, it would produce solutions which are unbounded in space (thus never solitons). Therefore, in order to illustrate the validity for this conclusion in the case of multiple zeros, we consider the second-order fundamental-soliton in the \mathcal{PT} -symmetric NLS equation by choosing a single pair of eigenvalues $(\zeta_1, \bar{\zeta}_1) \in i\mathbb{R}_+$ in expression (29), then it produces a high-order “fundamental-soliton”. Although it still satisfies eq.(1), this solution is not localized in space and grows exponentially in the positive x directions.

Acknowledgment

This project is supported by the Global Change Research Program of China (No.2015CB953904), National Natural Science Foundation of China (No.11675054 and 11435005), and Shanghai Collaborative Innovation Center of Trustworthy Software for Internet of Things (No. ZF1213).

References

- [1] M.J. Ablowitz and H. Segur, *Solitons and Inverse Scattering Transform* (SIAM, Philadelphia, 1981).
- [2] S. Novikov, S.V. Manakov, L.P. Pitaevskii and V.E. Zakharov, *Theory of Solitons* (Plenum, New York, 1984).
- [3] L. Takhtadjan and L. Faddeev, *The Hamiltonian Approach to Soliton Theory* (Springer Verlag, Berlin, 1987).
- [4] M.J. Ablowitz and P.A. Clarkson, *Solitons, Nonlinear Evolution Equations and Inverse Scattering* (Cambridge University Press, 1991).
- [5] J. Yang, *Nonlinear Waves in Integrable and Non integrable Systems* (SIAM, Philadelphia, 2010).
- [6] M. J. Ablowitz and Z. H. Musslimani, “Integrable nonlocal nonlinear Schrödinger equation”, *Phys. Rev. Lett.* 110, 064105 (2013).
- [7] M.J. Ablowitz and Z.H. Musslimani, “Inverse scattering transform for the integrable nonlocal nonlinear Schrödinger equation,” *Nonlinearity* 29, 915–946 (2016).
- [8] T.A. Gadzhimuradov and A.M. Agalarov, “Towards a gauge-equivalent magnetic structure of the nonlocal nonlinear Schrödinger equation, *Phys. Rev. A* 93, 062124 (2016).
- [9] V.V. Konotop, J. Yang and D.A. Zezyulin, “Nonlinear waves in \mathcal{PT} -symmetric systems,” *Rev. Mod. Phys.* 88, 035002 (2016).
- [10] M.J. Ablowitz and Z.H. Musslimani, “Integrable nonlocal nonlinear equations”, *Stud. Appl. Math.* 139(1), 7-59 (2016).
- [11] V. S. Gerdjikov and A. Saxena, “Complete integrability of nonlocal nonlinear Schrödinger equation”, *J. Math. Phys.* 58, 013502 (2017).
- [12] M.J. Ablowitz, X. Luo, and Z.H. Musslimani, “Inverse scattering transform for the nonlocal nonlinear Schrödinger equation with nonzero boundary conditions”, *arXiv:1612.02726 [nlin.SI]* (2016).
- [13] X. Y. Wen, Z. Yan and Y. Yang, “Dynamics of higher-order rational solitons for the nonlocal nonlinear Schrödinger equation with the self-induced parity-timesymmetric potential”, *Chaos* 26, 063123 (2016).
- [14] X. Huang and L. M. Ling, “Soliton solutions for the nonlocal nonlinear Schrödinger equation,” *Eur. Phys. J. Plus* 131, 148 (2016).
- [15] S. Stalin, M. Senthilvelan, and M. Lakshmanan, “Nonstandard bilinearization of \mathcal{PT} -invariant nonlocal Schrödinger equation: bright soliton solutions”, *Phys. Lett. A* 381, 2380-2385 (2017).
- [16] B. Yang and J. Yang, “General rogue waves in the \mathcal{PT} -symmetric nonlinear Schrödinger equation”, *arXiv:1711.05930 [nlin.SI]* (2017).
- [17] B. F. Feng, X. D. Luo, M. J. Ablowitz and Z. H. Musslimani, “General soliton solution to a nonlocal nonlinear Schrödinger equation with zero and nonzero boundary conditions”, *arXiv:1712.01181 [nlin.SI]* (2017).
- [18] Y. Rybalko and D. Shepelsky, “Long-time asymptotics for the integrable nonlocal nonlinear Schrödinger equation”, *arXiv:1710.07961 [nlin.SI]* (2017).

- [19] J. Yang, “General N-solitons and their dynamics in several nonlocal nonlinear Schrödinger equations”, arXiv:1712.01181 [nlin.SI] (2017).
- [20] K. Chen and D.J. Zhang, “Solutions of the nonlocal nonlinear Schrödinger hierarchy via reduction”, Appl. Math. Lett., 75, 82-88 (2018).
- [21] M. J. Ablowitz and Z. H. Musslimani, “Integrable discrete \mathcal{PT} -symmetric model”, Phys. Rev. E 90, 032912 (2014).
- [22] Z. Yan, “Integrable \mathcal{PT} -symmetric local and nonlocal vector nonlinear Schrödinger equations: A unified two-parameter model,” Appl. Math. Lett. 47, 61–68 (2015).
- [23] A. Khara and A. Saxena, “Periodic and hyperbolic soliton solutions of a number of nonlocal nonlinear equations”, J. Math. Phys. 56, 032104 (2015).
- [24] C Song, D. Xiao and Z. Zhu ”Reverse Space-Time Nonlocal Sasa-Satsuma Equation and Its Solutions.” Journal of the Physical Society of Japan 86 (2017).
- [25] B. Yang and J. Yang, “Transformations between nonlocal and local integrable equations”, Stud. Appl. Math. DOI: 10.1111/sapm.12195 (2017).
- [26] A.S. Fokas, “Integrable multidimensional versions of the nonlocal nonlinear Schrödinger equation”, Nonlinearity 29, 319–324 (2016).
- [27] S.Y. Lou and F. Huang, “Alice-Bob physics: coherent solutions of nonlocal KdV systems”, Scientific Reports 7, 869 (2017).
- [28] Z.X. Zhou, “Darboux transformations and global solutions for a nonlocal derivative nonlinear Schrödinger equation”, arXiv:1612.04892 [nlin.SI] (2016).
- [29] J.G. Rao, Y. Cheng and J.S. He, “Rational and semi-rational solutions of the nonlocal Davey-Stewartson equations”, Stud. Appl. Math. 139, 568–598 (2017).
- [30] B. Yang and Y. Chen, “Dynamics of Rogue Waves in the Partially \mathcal{PT} -symmetric Nonlocal Davey-Stewartson Systems”, arXiv:1710.07061 [math-ph] (2017).
- [31] J.L. Ji and Z.N. Zhu, “On a nonlocal modified Korteweg-de Vries equation: integrability, Darboux transformation and soliton solutions”, Commun. Nonlinear Sci. Numer. Simul. 42 699–708 (2017).
- [32] L.Y. Ma, S.F. Shen and Z.N. Zhu, “Soliton solution and gauge equivalence for an integrable nonlocal complex modified Korteweg-de Vries equation”, J. Math. Phys. 58, 103501 (2017).
- [33] M. Gürses, “Nonlocal Fordy-Kulish equations on symmetric spaces”, Phys. Lett. A 381, 1791-1794 (2017).
- [34] L. Gagnon and N. Stivenart “N-soliton interaction in optical fibers: the multiple-pole case”, Opt. Lett. 19, 619-621 (1994)
- [35] H. Tsuru and M. Wadati, “The Multiple Pole Solutions of the Sine-Gordon Equation”, J. Phys. Soc. Japan, 53, 2908-2921 (1984)
- [36] J. Villarroel and M. J. Ablowitz, “A novel class of solutions of the non-stationary Schrödinger and the Kadomtsev-Petviashvili I equations”, Commun. Math. Phys. 207, 1-42 (1999)
- [37] M. J. Ablowitz, S. Charkravarty, A. D. Trubatch and J. Villarroel, “On the discrete spectrum of the nonstationary Schrödinger equation and multipole lumps of the Kadomtsev-Petviashvili I equation”, Phys. Lett. A, 267, 132-146 (2000)

- [38] V.E. Zakharov and A.B. Shabat, "Exact theory of two-dimensional self-focusing and one-dimensional self-modulation of waves in nonlinear media", Zh. Eksp. Teor. Fiz. 61, 118 (1971) [Sov. Phys. JETP 34, 62 (1972)].
- [39] M.J. Ablowitz, D.J. Kaup, A.C. Newell and H. Segur, "The inverse scattering transform † Fourier analysis for nonlinear problems", Stud. Appl. Math. 53, 249 (1974)
- [40] V.E. Zakharov and A.B. Shabat, Integration of the nonlinear equations of mathematical physics by the method of the inverse scattering problem II, Funk. Anal. Prilozh. 13, 13-22 (1979) [Funct. Anal. Appl. 13, 166-174 (1979)].
- [41] V.S. Shchesnovich and J. Yang, General soliton matrices in the Riemann-Hilbert problem for integrable nonlinear equations. J. Math. Phys. 44, 4604-4639 (2003).
- [42] D. Bian, B. L. Guo and L. M. Ling. "High-Order Soliton Solution of Landau-Lifshitz Equation," 2015 Stud. Appl. Math. 134, 181–214.